RSC Advances

The *cis*- and *trans*-formylperoxy radical: Fundamental vibrational frequencies and relative energies of the X ^{2}A'' and A ^{2}A' states

Journal:	*RSC Advances*
Manuscript ID	RA-ART-10-2015-022177.R1
Article Type:	Paper
Date Submitted by the Author:	24-Nov-2015
Complete List of Authors:	Elliott, Sarah; University of Georgia, Computational Chemistry Turney, Justin; University of Georgia, Center for Computational Chemistry Schaefer, Henry; University of Georgia, Computational Chemistry
Subject area & keyword:	Quantum & theoretical < Physical

Journal Name

ARTICLE TYPE

Cite this: DOI: 10.1039/xxxxxxxxxx

The *cis*- and *trans*-formylperoxy radical: Fundamental vibrational frequencies and relative energies of the $\tilde{X}\,^2A''$ and $\tilde{A}\,^2A'$ states

Sarah N. Elliott,[a] Justin M. Turney,[a] and Henry F. Schaefer*[a]

Received Date
Accepted Date

DOI: 10.1039/xxxxxxxxxx

www.rsc.org/journalname

Acylperoxy radicals [RC(O)OO•] play an important catalytic role in many atmospheric and combustion reactions. Accordingly, the prototypical formylperoxy radical [HC(O)OO•] is characterized here using high-level *ab initio* coupled-cluster theory. Important experiments have been carried out on this system, but have not comprehensively described the properties of even the ground electronic state. We report *cis* and *trans* geometries for the ground ($\tilde{X}\,^2A''$) and first excited ($\tilde{A}\,^2A'$) state equilibrium conformers and the torsional saddle point on the ground state surface at the CCSD(T)/ANO2 level of theory. Relative energies of these ground- and excited-state stationary points were obtained using coupled cluster theory with up to perturbative quadruple excitations, extrapolated from the sextuple zeta basis set to the complete basis set limit. These methods predict conformational energy differences $\Delta E(trans\text{-}\tilde{X}\rightarrow cis\text{-}\tilde{X})$ = 2.35 kcal mol^{-1} and $\Delta E(trans\text{-}\tilde{A}\rightarrow cis\text{-}\tilde{A})$ = −2.95 kcal mol^{-1}. On the $\tilde{X}$ surface, the transition state for the conformational change lies 8.42 kcal mol^{-1} above the *trans* ground state minima. The adiabatic electronic excitation energies from the ground state isomers are predicted to be 18.17 ± 0.10 (*trans*) and 13.03 ± 0.10 kcal mol^{-1} (*cis*). The former is in excellent agreement with the 18.1 ± 1.4 kcal mol^{-1} transition found by Lineberger and coworkers. Additionally, transition properties between the $\tilde{X}\,^2A''$ and $\tilde{A}\,^2A'$ states are reported for the first time, using the equation of motion (EOM)-CCSD method, which predicts lifetimes for *trans*-$\tilde{A}\,^2A'$ HC(O)OO• of 5.4 ms and *cis*-$\tilde{A}\,^2A'$ HC(O)OO• of 20.5 ms. Second-order vibrational perturbation theory was utilized to determine the fundamental frequencies at the CCSD(T)/ANO2 level of theory for the *cis* and *trans* conformers of the $\tilde{X}$ and $\tilde{A}$ states and five ground state isotopologues of both conformers: H^{13}C(O)OO•, HC(^{18}O)OO•, HC(O)^{18}O^{18}O•, DC(O)OO•, and DC(O)^{18}O^{18}O•. This study provides high accuracy predictions of vibrational frequencies, helping to resolve large uncertainties and disagreements in the experimental values. Furthermore, we characterize experimentally unassigned vibrational frequencies and transition properties.

1 Introduction

The formyl radical (HC•O) is a chain branching intermediate produced during methane oxidation, a common process in fuel combustion and in the lower atmosphere. In the early stages of the oxidative process, HC•O is formed from formaldehyde – either by photodissociation, or via reaction with a variety of open-shell species.[1–5] The nature of formyl radical reactivity is relevant to understanding atmospheric chemistry in polluted environments due to its liberation of H• to yield CO and the reaction of H•CO with O_2 to furnish HO_2•. The current research is concerned with characterization of the formylperoxy radical, an intermediate in the latter reaction, shown explicitly below (Reaction R1).[2,4]

$$HC^{\bullet}O + O_2 \longrightarrow [HC(O)OO^{\bullet}] \longrightarrow HO_2^{\bullet} + CO \qquad (R1)$$

Interest in R1 is derived from the harmful effects of its product HO_2•, which is known to propogate photochemical smog throughout the troposphere.[6,7]

Osif and Heicklen (1976) were the first to experimentally investigate HC(O)OO• as an intermediate in R1 (Ref. 8) following observation of the HO_2• product via laser magnetic resonance spectroscopy of formyl radical oxidation.[9] Their support of an HC(O)OO• intermediate, through gas chromotography monitored formaldehyde irradiation, was quickly followed by both spectroscopic and theoretical reports.[10–12] Infrared spectroscopy on formaldehyde in solid oxygen displayed absorption peaks at

[a] Center for Computational Quantum Chemistry, University of Georgia, Athens, Georgia 30602, USA. Fax: +1 (706) 542-0406; Tel: +1 (706) 542-2067; E-mail: ccq@uga.edu

1790 and 1090 cm^{-1}.[10] The experimentalists, Lee and Diem, attributed these peaks to HC(O)OO$^\bullet$ formed during reaction R1. Unscaled restricted Hartree Fock (RHF) computations with the 6-31G(*d,p*) basis set found these to originate from the C=O and C–O stretching motions of *trans*-HC(O)OO$^\bullet$.[11]

These early results concerning R1 were expanded upon using the G2M restricted coupled cluster (RCC) composite method, along with Rice-Ramsperger-Kassel-Marcus (RRKM) theory for kinetic rate predictions.[13] Hsu, Mebel, and Lin concluded that the major channel proceeds through the *trans*-HC(O)OO$^\bullet$ association product in a concerted manner to $HO_2^\bullet$ and CO.[12–15] Alternatively, the hydrogen of *trans*-HC(O)OO$^\bullet$ may migrate from the carbon to the terminal oxygen, forming an $^\bullet$C(O)OOH transition state, before dissociating to CO_2 and HO$^\bullet$ or, 35 kcal mol^{-1} less favorably, to $HO_2^\bullet$ and CO$^\bullet$ (R2).

$$\tilde{X}\,^2A'' \text{ HC(O)OO}^\bullet \longrightarrow {}^\bullet\text{C(O)OOH} \longrightarrow CO_2 + HO^\bullet \qquad \text{(R2)}$$
$$\longrightarrow CO + HO_2^\bullet$$

Though the barrier for the CO_2 and HO$^\bullet$ reaction is high, the 36 kcal mol^{-1} exothermic formation of the HC(O)OO$^\bullet$ is assumed to be sufficiently energetic to drive the reaction (possibly after progressing back through the hydroperoxo-oxomethyl radical complex).[14,16–18] Reactions of the hydrogen migration product, hydroxyformyl radical [$^\bullet$C(O)OOH], are pivotal to low temperature autoignition chemistry,[19] and the hydroxyl radical (HO$^\bullet$) has been identified as the most important intermediate in the consumption of olefins in the atmosphere.[7]

By 1975, Winter and Goddard[20] had already proposed a different possibility for the reaction of HCO and O_2; the association may be sufficiently exothermic for internal conversion to the first excited state ($\tilde{A}\,^2A'$) HC(O)OO$^\bullet$. Upon formation, the *trans*-$\tilde{A}\,^2A'$ state of HC(O)OO$^\bullet$ undergoes a highly exothermic (−54 kcal mol^{-1}) decomposition (R3) to CO_2 and HO$^\bullet$.

$$\tilde{A}\,^2A' \text{ HC(O)OO}^\bullet \longrightarrow CO_2 + HO^\bullet \qquad \text{(R3)}$$

The close energy spacing between the $\tilde{X}$ and $\tilde{A}$ states of peroxy radicals often necessitates examination of both electronic states.

Within the last decade, the HC(O)OO$^\bullet$ radical has been further characterized experimentally and qualitatively using density functional theory (DFT). Formylperoxy radical may exist in two conformers, with the terminal oxygen either *trans* or *cis* to the carbonyl. The *trans* isomer was predicted to be 1.9 kcal mol^{-1} lower in energy than the *cis*, with a barrier height of 8.8 kcal mol^{-1} at the B3LYP/6-311++G(*d,p*) level at 0 K.[16] To ensure that $HO_2^\bullet$ was not present in their characterization of HC(O)OO$^\bullet$, which they suspected of earlier studies, Yang, Yu, Zeng and Zhou[21] reported the infrared spectra and vibrational frequency assignments of the formylperoxy radical in an argon matrix. Aided by B3LYP and MP2 calculations with the 6-311++G(*d,p*) basis, Yang et al. reported the experimental C=O and C−O stretching vibrations to be 1821.5 and 957.3 cm^{-1}, and attributed them to the *trans* isomer. Recently, the isolated formylperoxy radical has been studied experimentally by Villano, Eyet, Wren, Ellison, Bierbaum, and Lineberger.[22] Gas phase measurements have been made via photodetachment from the formylperoxy anion.[22] The experimental ν_4, ν_5, and ν_6 frequencies were found to be 1098 ± 20, 973 ± 20, and 574 ± 35 cm^{-1}, respectively and were assigned to the *trans* isomer. The gap between experimental and previous results is ≥50 cm^{-1} for several fundamentals. That, combined with the large uncertainty in the four experimentally measured frequencies, calls for a higher level theoretical study.

Ever-increasing interest in peroxyacyl systems provides additional motivation for HC(O)OO$^\bullet$ study. This class of molecules plays a large role in the distribution of oxygen, ozone, hydroxyl radical, and $NO_x^\bullet$ in the atmosphere.[23] Distinct from alkylperoxy radicals, peroxyacyl radicals offer inductive stabilization by the carbonyl group to peroxyacyl nitrates, facilitate HO$^\bullet$ recycling via the carbonyl oxygen, and are more abundant in the atmosphere. These attributes make the characterization of acylperoxy radicals critical to atmospheric chemistry.

Herein, we provide a characterization of the ground-state conformers of the formylperoxy radical and their $\tilde{A} \leftarrow \tilde{X}$ excitation products using high-level *ab initio* methods. The relative energies of the *cis* and *trans* conformers, and the barrier height to interconversion between them, are predicted using coupled-cluster (CC) methods extrapolated to the complete basis set (CBS) limit. Anharmonic vibrational frequencies of both structures in the ground and first excited states, including various isotopologues of the ground state, are computed for the first time, using coupled-cluster methods with second-order vibrational perturbation theory (VPT2). The structures of the excitation products of the *cis* and *trans* rotamers, their transition properties, as well as adiabatic excitation energies extrapolated to the CBS limit, are also reported.

2 Theoretical Methods

Computations were performed using the CFOUR,[24,25] MRCC,[26] and PSI4 (Ref. 27) programs. At the coupled cluster singles, doubles, and perturbative triples [CCSD(T)] level of theory, optimized geometries were determined for the *cis* and *trans* conformers in both the $\tilde{X}\,^2A''$ and $\tilde{A}\,^2A'$ states. These computations employed the correlation-consistent polarized-valence quadruple zeta (cc-pVQZ) basis sets of Dunning.[28] Concurrently, the full atomic natural orbital (ANO) basis set of Almlöf and Taylor, ANO2, geometries were obtained for the vibrational frequency computations.[29] The ANO sets, while sharing nearly identical Gaussian function contraction patterns, have greater numbers of primitive functions for *sp* and polarization functions than the comparably sized Dunning basis sets. These basis set have been found to outperform correlation consistent basis sets for some vibrational frequencies.[30]

In all cases, an unrestricted Hartree-Fock (UHF) determinant was used as the reference wave function, which allowed for the use of analytic second derivatives in vibrational frequency computations.[31] The accuracy of this reference is influenced by the degree of spin-contamination and static correlation in the system. The commonly used $\mathscr{T}_1$ diagnostic[32–34] analogizes the magnitude of orbital-relaxation effects in the CCSD wave function to multireference requirements, and sometimes advises a multiref-

erence approach for $\mathscr{T}_1 > 0.02$. While each of the conformers for the formylperoxy radical have $\mathscr{T}_1 = 0.05$ (see Table 1), for open-shell systems the $\mathscr{T}_1$ diagnostic has a less well-defined threshold. This is because large orbital-relaxation effects may be attributed to dynamic correlation rather than the static correlation.[35] Instead, the largest T_2 amplitude (max t_{ij}^{ab}) has been found to be a better description of the character of these systems.[35] The max t_{ij}^{ab} of $0.04-0.05$, and the $\langle \hat{S}^2 \rangle_{\mathrm{UHF}}$ values of 0.76 for each system (which have minimal deviation from the expected value of 0.75 for a doublet state) indicate that the wave function is sufficiently described to the zeroth order by a single UHF reference determinant.

Table 1 Diagnostics on the single reference UHF determinant for the isomers of formylperoxy radical. With $\mathscr{T}_1 = \sqrt{\frac{|t_1^{\alpha\alpha}|^2 + |t_1^{\beta\beta}|^2}{N_{\mathrm{corr}}}}$ and max t_{ij}^{ab} is the maximum value in the T_2 amplitudes.

	$\tilde{\mathrm{X}}$ ^{2}A″			$\tilde{\mathrm{A}}$ ^{2}A′	
	trans	*cis*	TS	*trans*	*cis*
$\langle \hat{S}^2 \rangle_{UHF}$	0.76	0.76	0.76	0.76	0.76
$\mathscr{T}_1$	0.040	0.039	0.042	0.034	0.032
max t_{ij}^{ab}	0.05	0.05	0.04	0.05	0.05

Relative energies of the optimized structures were obtained by the focal point approach (FPA)[36–39] – a convergent scheme in which both electron correlation and basis set limits are systematically approached. The correlation treatment was extended as far as the CCSDT(Q) method,[26,40,41] which includes contributions from quadruple excitations analogous to the triples term in the popular CCSD(T) theory. Basis set extrapolation to the CBS limit was performed by applying a three-parameter exponential function for the Hartree Fock energy

$$E_X^{\mathrm{HF}} = E_{\mathrm{CBS}}^{\mathrm{HF}} + ae^{-bX} \quad (1)$$

and a two-term form for the correlation energy

$$E_X^{\mathrm{corr}} = E_{\mathrm{CBS}}^{\mathrm{corr}} + aX^{-3} \quad (2)$$

to single-point energies computed with the cc-pVXZ (X = D, T, Q, 5, 6) family of basis sets.[28] The Dunning basis sets were selected due to their facilitation toward convergence. The frozen-core approximation was utilized in all optimizations. Core correlation corrections to the energies were computed as:

$$\Delta E_{\mathrm{core}} = E_{\mathrm{CCSD(T)(AE)}}^{\mathrm{cc\text{-}pCVQZ}} - E_{\mathrm{CCSD(T)(FC)}}^{\mathrm{cc\text{-}pCVQZ}} \quad (3)$$

where AE and FC notate all electron and frozen core. Including one- and two-electron Darwin terms and mass velocity contributions[42,43] accounted for scalar relativistic effects at first order. These were obtained at the all-electron CCSD(T)/aug-cc-pCVTZ level, as advocated for first row atoms.[44,45] As a test for non-adiabatic effects, we used the diagonal Born-Oppenheimer correction (DBOC) computed at HF/aug-cc-pVTZ.[46,47]

Harmonic vibrational frequencies were determined analytically at the CCSD(T)/ANO2 level of theory. Second order vibrational perturbation theory (VPT2) was used to compute anharmonic corrections ($\delta\nu$) with the CCSD(T)/ANO1 method. The VPT2 method employs the full cubic force field and the semi-diagonal part of the quartic force field. These force fields were ascertained via numerical differentiation of the harmonic frequencies with respect to normal coordinates. We also include a correction for orbital-relaxation effects ($\delta\omega$), computed as the difference between Brueckner-[48,49] and CCSD(T)/ANO1 harmonic frequencies. Addition of these corrections to CCSD(T)/ANO2 harmonic vibrational frequencies (ω) resulted in final frequencies (ν), $\nu = \omega + \delta\omega + \delta\nu$. These geometries and frequencies were obtained via single-point energy computations interfaced with PSI4's optimization and finite-difference codes.[27]

3 Results and Discussion

3.1 Geometries

The formylperoxy radical has two conformers which are labeled *cis* and *trans* based on the orientation of the O′O″ bond with respect to the carbonyl (see Figure 1). Each has an electron configuration in the ground state of $(1a')^2(2a')^2\cdots(13a')^2(3a'')$. The term symbols for the ground ($\tilde{\mathrm{X}}$) and first excited ($\tilde{\mathrm{A}}$) states are ^{2}A″ and ^{2}A′, respectively. Figure 2 depicts the the $13a'$ and $3a''$ orbitals, which correspond predominantly to the in-plane and out-of-plane π^* orbitals of O_2.

Figures 1a and 1b show the optimized geometries for the $\tilde{\mathrm{X}}$ ^{2}A″ *cis* and *trans* isomers computed at the CCSD(T)/ANO2 and CCSD(T)/cc-pVQZ levels of theory. The *trans-cis* internal rotation transition state optimization in CFOUR applied the Cerjan-Miller method,[?] and harmonic vibrational analysis verified the saddle point structure (Figure 1c). The $\tilde{\mathrm{A}}$ ^{2}A′ *cis* and *trans* isomers optimized geometries, at the same levels, are shown in Figures 1c and 1d. Optimized geometries for both basis sets agree to within 0.001 Å for all bond lengths and 0.1° for all angles. The excited states are structurally similar to the ground state geometries, but are distinguished in both conformers by a 0.06 Å elongation of the O′O″ bond and 0.03 Å contraction of the CO bond. In the *trans* isomer, the HCO′ and CO′O″ angles increase by about 3° each from the ^{2}A″ to the ^{2}A′ state at the expense of the OCO′ angle. In contrast, the angles of the *cis* isomer, constrained by the interaction between the carbonyl oxygen and terminal peroxy oxygen, are not significantly affected by excitation of an electron from the lone pair (lp) to the singly occupied out-of-plane π^* orbital (lp $\rightarrow \pi^*$).

The significant elongation of the O−O bond distance between structures of the ground and first-excited states is characteristic of the $\tilde{\mathrm{X}}$ and $\tilde{\mathrm{A}}$ states of RO_2 species and has been theoretically recognized in similar systems [$C_2H_5O_2^{\bullet}$, $CH_3O_2^{\bullet}$,$CH_3C(O)O_2^{\bullet}$, and $HO_2^{\bullet}$].[35,50–52] Our O−O equilibrium distances are roughly 1.33 Å for the ground state stationary points (Figs. 1a-c), considerably shorter than the ≈1.39 O−O Å bond found for the excited state structures (Figs. 1d and 1e). The O−O bond lengths match the related theoretical $\tilde{\mathrm{A}}$ and $\tilde{\mathrm{X}}$ $CH_3C(O)O_2^{\bullet}$ lengths (to within 0.002 Å and 0.008 Å, respectively).[35] Comparing to the peroxyl bonds of HO_2 (Ref. 53) reveals the computed $\tilde{\mathrm{X}}$ and $\tilde{\mathrm{A}}$ HC(O)OO peroxyl bond lengths differ from experiment by only 0.001 Å and 0.01 Å. This experimental molecular geometry was determined from the rotational constants measured in the reaction of O/O_2

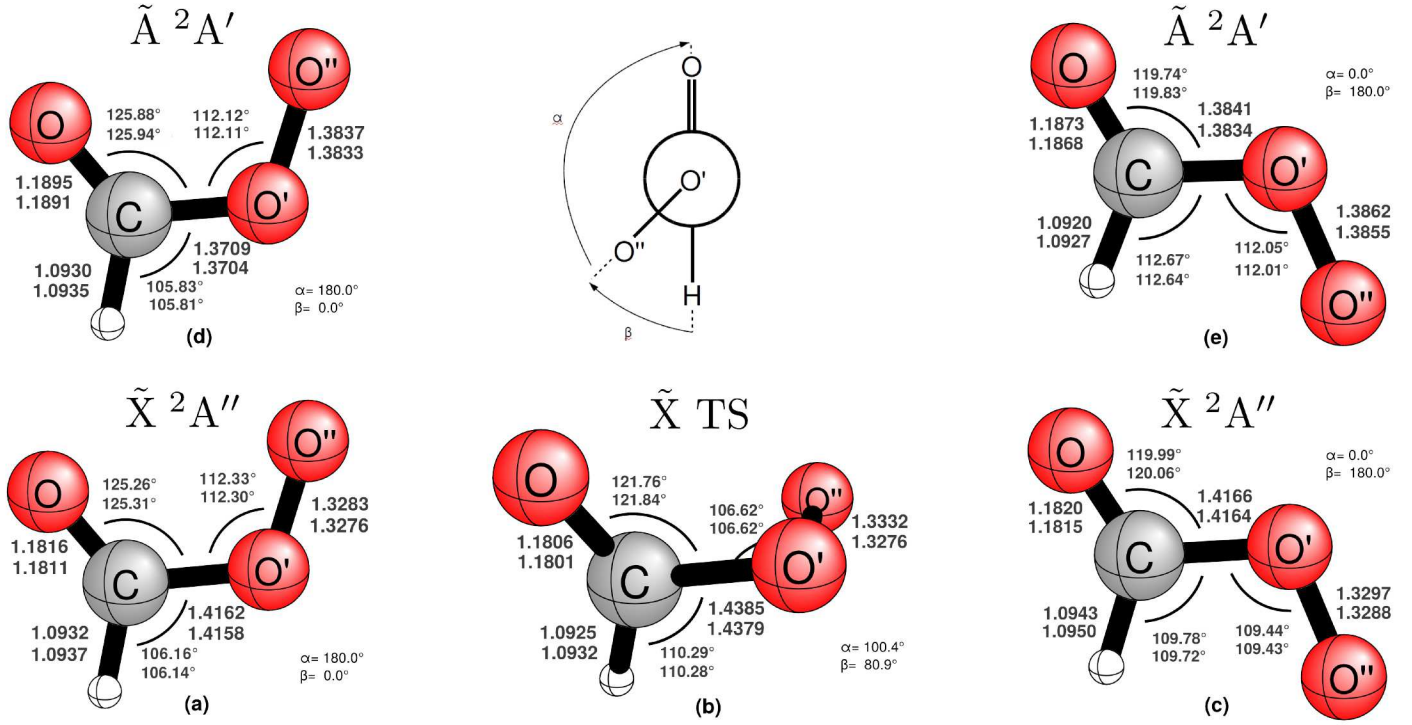

Fig. 1 The CCSD(T)/ANO2 (top) and CCSD(T)/cc-pVQZ (bottom) optimized geometries for (a) the $\tilde{X}\,^2A''$ *cis* structure; (b) the $\tilde{X}$ torsional transition state (c) the $\tilde{A}\,^2A'$ *cis* structure; (d) the $\tilde{X}\,^2A''$ *trans* structure; and (e) the $\tilde{A}\,^2A'$ *trans* structure.

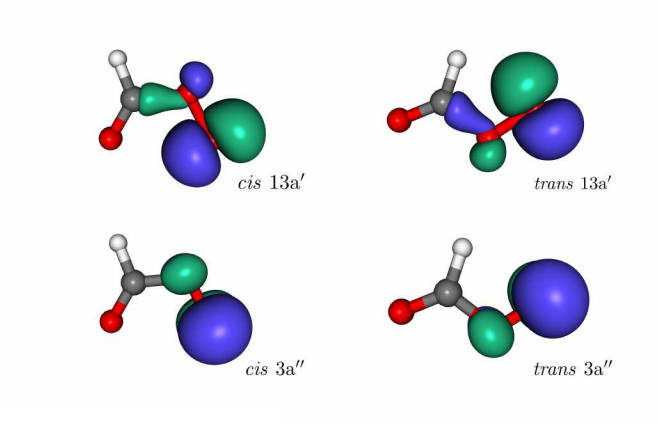

Fig. 2 CASSCF/cc-pVDZ ground and first excited state averaged 13a' and 3a'' orbitals (the HOMO and SOMO, respectively) for HC(O)OO•.

and CD_3OD or CH_3OH in a discharge flow system. Tuckett, Freedman, and Jones used interferometric spectrometry to determine the constants by an independent state fit of the combination differences in the spectra of HO_2 and DO_2.

3.2 Relative Energies

To further characterize the $\tilde{X}$ and $\tilde{A}$ potential energy surfaces of formylperoxy radical, we computed the thermodynamic relationships between all of the conformers in Figure 1. In particular, we have determined relative electronic energies utilizing the CCSD(T)/cc-pVQZ geometries and using coupled-cluster theory with up to perturbative quadruple excitations [CCSDT(Q)], extrapolated to the CBS limit. The relative energy between the *cis* and *trans* ground state conformers is shown in Table 2. Excellent convergence emerges in the focal-point treatment, using up to the cc-pV6Z basis set. Here, basis set uncertainty is 0.01 kcal mol^{-1} on the ground state surface and 0.02 kcal mol^{-1} on the excited state surface at CCSDT(Q). Similarly, the correlation treatment converges towards the full CI limit very nicely. Contributions of perturbative quadruples at the CBS limit are 0.01 (for the *trans*-$\tilde{X}\,^2A'' \rightarrow$ *cis*-$\tilde{X}\,^2A''$ transition), 0.02 (for the *trans*-$\tilde{X}\,^2A'' \rightarrow \tilde{X}$ TS), 0.04 (for the *trans*-$\tilde{X}\,^2A'' \rightarrow$ *trans*-$\tilde{A}\,^2A'$), 0.08 (for the *cis*-$\tilde{X}\,^2A'' \rightarrow$ *cis*-$\tilde{A}\,^2A'$), and 0.05 kcal mol^{-1} (for the *trans*-$\tilde{A}\,^2A' \rightarrow$ *cis*-$\tilde{A}\,^2A'$). Bearing in mind both the basis set and correlation uncertainties, the estimated uncertainty to the final energy (Δ_e) for all structures is within thermochemical accuracy (0.1 kcal mol^{-1}).[54] Focal point treatment of the ground state relative energy between the CCSD(T)/ANO2 conformers resulted in the same basis set and correlation uncertainties as well as the same final electronic energy as for the CCSD(T)/cc-pVQZ.

Core (Δ_{core}), relativistic (Δ_{rel}), and non-adiabatic (Δ_{DBOC}) corrections are shown in Table 3. These considerations affect the final energies by 0.00–0.04 kcal mol^{-1}, indicating that the corresponding approximations are appropriate for this system. Anharmonic zero-point vibrational energies (Δ_{ZPVE}) were computed using Equations 3 and 4 of Ref. **?** with CCSD(T)/cc-pVQZ harmonic force constants and CCSD(T)/ANO1 cubic and quartic force constants. The values range from 0.04–0.26 kcal mol^{-1} (Table 3).

The final, corrected relative energies (ΔH_{0K}) are given in Table 3 and shown schematically in Figure 3. It is interesting to note that whereas the *trans* isomer is predicted to lie 2.41 kcal mol^{-1} lower in energy than the *cis* isomer, the energetic ordering is reversed in the excited state, where the *cis*-$\tilde{A}\,^2A'$ conformer is 2.73

Table 2 Relative electronic energies (kcal mol^{-1}) for formylperoxy radical conformers extrapolated to the complete basis set limit [CCSDT(Q)/CBS].

			Coupled-Cluster				
n	UHF	δMP2	δSD	δSD(T)	δSDT	δSDT(Q)	SDT(Q)
1. Ground state							
			trans ($\tilde{X}$ A″) → *cis* ($\tilde{X}$ A″)				
D	+0.35	+1.47	–0.13	+0.08	+0.07	+0.01	+1.85
T	+0.93	+1.42	–0.19	+0.12	+0.04	+0.01	+2.33
Q	+1.04	+1.39	–0.20	+0.12	[+0.04]	[+0.01]	[+2.40]
5	+1.04	+1.35	–0.20	+0.11	[+0.04]	[+0.01]	[+2.36]
6	+1.05	+1.34	[–0.20]	[+0.11]	[+0.04]	[+0.01]	[+2.36]
∞	[+1.05]	[+1.33]	[–0.20]	[+0.11]	[+0.04]	[+0.01]	**[+2.35]**
2. Isomerization barrier							
			trans ($\tilde{X}$ A″) → $\tilde{X}$ TS				
D	+9.58	+0.31	–1.09	+0.14	+0.01	–0.01	+8.93
T	+9.70	+0.12	–0.99	+0.07	+0.01	–0.02	+8.89
Q	+9.74	+0.11	–0.96	+0.04	[+0.01]	[–0.02]	[+8.92]
5	+9.74	+0.09	–0.95	+0.03	[+0.01]	[–0.02]	[+8.88]
6	+9.74	+0.09	[–0.95]	[+0.03]	[+0.01]	[–0.02]	[+8.88]
∞	[+9.74]	[+0.09]	[–0.95]	[+0.03]	[+0.01]	[–0.02]	**[+8.89]**
3. Adiabatic excitation energies							
			trans ($\tilde{X}$ A″) → *trans* ($\tilde{A}$ A′)				
D	+13.23	+4.82	–0.27	+0.26	–0.10	+0.03	+17.98
T	+13.14	+4.93	–0.34	+0.46	–0.16	+0.04	+18.06
Q	+13.21	+5.05	–0.34	+0.49	[–0.16]	[+0.04]	[+18.30]
5	+13.21	+5.09	–0.34	+0.51	[–0.16]	[+0.04]	[+18.34]
6	+13.21	+5.11	[–0.34]	[+0.51]	[–0.16]	[+0.04]	[+18.36]
∞	[+13.21]	[+5.13]	[–0.34]	[+0.51]	[–0.16]	[+0.04]	**[+18.38]**
			cis ($\tilde{X}$ A″) → *cis* ($\tilde{A}$ A′)				
D	+8.48	+3.88	+0.25	+0.32	–0.04	+0.06	+12.96
T	+8.29	+3.83	+0.23	+0.50	–0.06	+0.08	+12.86
Q	+8.33	+3.91	+0.24	+0.53	[–0.06]	[+0.08]	[+13.02]
5	+8.32	+3.93	+0.24	+0.55	[–0.06]	[+0.08]	[+13.06]
6	+8.32	+3.95	[+0.24]	[+0.55]	[–0.06]	[+0.08]	[+13.07]
∞	[+8.31]	[+3.97]	[+0.25]	[+0.56]	[–0.06]	[+0.08]	**[+13.09]**
4. Excited state relative energies							
			cis ($\tilde{A}$ A′) → *trans* ($\tilde{A}$ A′)				
D	+4.40	–0.53	–0.39	–0.14	–0.14	–0.04	+3.16
T	+3.93	–0.33	–0.39	–0.16	–0.13	–0.05	+2.88
Q	+3.85	–0.25	–0.39	–0.16	[–0.13]	[–0.05]	[+2.88]
5	+3.85	–0.19	–0.39	–0.15	[–0.13]	[–0.05]	[+2.92]
6	+3.84	–0.18	[–0.39]	[–0.15]	[–0.13]	[–0.05]	[+2.93]
∞	[+3.84]	[–0.17]	[–0.39]	[–0.15]	[–0.13]	[–0.05]	**[+2.95]**

Brackets indicate values obtained by extrapolations or additivity assumptions rather than direct computations. Final CCSDT(Q)/CBS values are shown in bold. The column labeled n refers to the cardinality of the basis set, cc-pVXZ, where $X = \infty$ is the CBS limit.

kcal mol^{-1} lower in energy than the *trans*-$\tilde{A}^2A'$. One possible explanation for this difference is that the long-range interaction between the terminal oxygens of the O=COO$^\bullet$ back-bone is repulsive when the 13a′ in-plane orbital (see Figure 2) is doubly occupied. This effect favors the *trans* conformer of the ground electronic state. The interaction is less repulsive when the 13a′ orbital is only singly occupied, favoring the *cis* conformer, in the excited state.

The energy of the *trans*-$\tilde{X}^2A'' \rightarrow$ *trans*-$\tilde{A}^2A'$ excitation has been measured to be 18.1 ± 1.4 kcal mol^{-1} using photoelectron spectroscopy by Lineberger and coworkers[22]. They identified this value via a 3.27 eV electron binding energy peak in the photoelectron spectrum that could be assigned only to *trans*-$\tilde{A}^2A'$ HC(O)OO. The uncertainty is due to their inability to distinguish if the peak (which is 18.0 kcal mol^{-1} higher than the 2.48 eV ground state band origin) was from the *trans*-$\tilde{A}^2A'$ CO′O″ bend or electronic band origin. We predict the *trans*-$\Delta H_{0K,\tilde{A}\leftarrow\tilde{X}}$ to be 18.17 ± 0.1 kcal mol^{-1}, well within the error bars of the experimental value. The *cis* isomer of the formylperoxy radical has yet to be detected, though the reaction barrier $\Delta H_{0K,cis-\tilde{X}\leftarrow trans-\tilde{X}}$ is determined in this work to be only 8.42 kcal mol^{-1}.

Vertical transition properties for *cis* and *trans* $\tilde{A} \leftarrow \tilde{X}$ were computed with the EOM-CCSD/ANO2 method (Table 4). The $\tilde{X}^2A''$ state equilibrium geometries were used for the purpose of finding absorption properties. The reciprocal of Einstein's transition probability coefficient ($\mathscr{A}$) is the maximum possible mean lifetime for a given state, when the only mechanism of deactivation is spontaneous emission to the lower state.[55] In this manner, the *trans* excited state lifetime is predicted to be $\tau_{\tilde{A}} \approx 5.4$ ms and the *cis* excited state has $\tau_{\tilde{A}} \approx 20.5$ ms. Neither the *cis* nor *trans* $\tilde{A}^2A'$ electronic state lifetime has yet been observed experimentally.

3.3 Fundamental Vibrational Analysis

VPT2 anharmonic frequencies for the $\tilde{X}^2A''$ *trans* and *cis* isomers are shown in Table 5 and illustrated in Figure 4. The most intense peak is the $\nu_2(a')$ C=O stretch (240 km mol^{-1} *trans*/ 197 km mol^{-1} *cis*) followed by the $\nu_5(a')$ C–O′ stretch (226 km mol^{-1}

Table 3 Enthalpies (H_{0K}) at 0 K from the addition of auxiliary core [CCSD(T)/cc-pCVQZ] (Δ_{core}), one and two-electron Darwin and mass velocity relativistic [CCSD(T)/aug-cc-pCVTZ] (Δ_{rel}), diagonal Born-Oppenheimer [HF/aug-cc-pVTZ] (Δ_{DBOC}), and anharmonic zero-point vibrational energy [CCSD(T)/cc-pVQZ] (Δ_{ZPVE}) corrections to the energy extrapolated to the CBS limit (E_{CBS}). All values are in kcal mol^{-1}.

	E_{CBS}	Δ_{core}	Δ_{rel}	Δ_{DBOC}	Δ_{ZPVE}	H_{0K}
cis ($\tilde{X}$ A″) → *trans* ($\tilde{X}$ A″)	2.35	−0.01	0.00	0.01	0.06	2.41
trans ($\tilde{X}$ A″) → $\tilde{X}$ TS	8.89	0.01	0.00	0.01	−0.49[a]	8.42
trans ($\tilde{X}$ A″) → *trans* ($\tilde{A}$ A′)	18.38	0.02	0.00	0.00	−0.24	18.17
cis ($\tilde{X}$ A″) → *cis* ($\tilde{A}$ A′)	13.09	0.02	−0.05	0.00	−0.04	13.03
trans ($\tilde{A}$ A′) → *cis* ($\tilde{A}$ A′)	2.95	−0.01	0.05	−0.01	−0.26	2.73

[a] The reported value does not include anharmonic contributions, as the transition state was not amenable to VPT2 treatment.

Table 4 Transition properties for $\tilde{A}\,^2A' \leftarrow \tilde{X}\,^2A''$ predicted at the EOM-CCSD/ANO2 level of theory. The quantity $\tilde{\nu}_A$ is the vertical excitation energy in kcal mol^{-1}, $|\langle\tilde{X}|\hat{\mu}|\tilde{A}\rangle|$ is the transition dipole moment in Debye, f_A is the oscillator strength, and the Einstein Coefficients $\mathscr{A}$ and $\mathscr{B}$ are given in units of Hz and m^3 J^{-1} s^{-2}, respectively.

	trans		*cis*	
	$\tilde{X}$ A″	$\tilde{A}$ A′	$\tilde{X}$ A″	$\tilde{A}$ A′
$\tilde{\nu}_A$	20.61	16.96	14.90	11.65
$\lvert\langle\tilde{X}\lvert\hat{\mu}\rvert\tilde{A}\rangle\rvert$	0.065	0.053	0.057	0.048
f_A	14.2×10^{-6}	7.8×10^{-6}	8.0×10^{-6}	4.4×10^{-6}
Coeff.	$\mathscr{B}=7.92\times10^{16}$	$\mathscr{A}=184$	$\mathscr{B}=6.11\times10^{16}$	$\mathscr{A}=48.8$

trans/ 182 km mol^{-1} *cis*). For the ground state conformers, the *cis* O′–O″ stretch is significantly greater in intensity than the *trans* (26 km mol^{-1} *trans*/ 75 km mol^{-1} *cis*). Table 5 provides frequencies for the excited $\tilde{A}\,^2A'$ state as well. The O′–O″ stretching fundamental displays the greatest change relative to the ground state – nearly 200 cm^{-1} lower in the excited state for both conformers. The red-shift is characteristic of (lp→ π^*) excitation. The increase in antibonding character weakens the bond, lowering the vibrational frequency.

Our predicted $\tilde{X}\,^2A''$ fundamental frequencies are consistent with experiment, as shown in Table 6. Comparing this work to experimental results supports previous claims[21,22] that, to date, all experimentally observed bands are those of the *trans* isomers. Only the ν_2, ν_4, ν_5, and ν_6 modes have been identified experimentally. The ν_2 (1790.2 cm^{-1}) and ν_5 (1089.9 cm^{-1}) stretches were determined by Tso and Lee[56] via UV photooxidation of solid O_2 *trans*-$H_2C_2O_2$ at 13K. Tso and Lee concluded that these features may not represent isolated HC(O)OO•, because the latter may complex to both HO_2 and CO. Yang et al. provide more reliable results for ν_2 (1821.5 cm^{-1}) and ν_5 (957.3 cm^{-1}) through solid Ar matrix isolation infrared spectroscopy. They suggested that the discrepancy between the two experimental results is due to their successful isolation of HC(O)OO• by condensation of CH_3OH/Ar and O_2/Ar via high-frequency discharge.[21] For the protonated species [HC(O)OOH], the Ar matrix shift for C=O is 7 cm^{-1}, O−O is 11 cm^{-1}, and C−O is 2 cm^{-1}.[57]. With a 13 cm^{-1} divergence from the Ar measurement,[21] our prediction for *trans*-$\tilde{X}\,^2A''$ ν_2 (1835 cm^{-1}) is within the standard deviation of Ar matrices (16 cm^{-1}),[58] albeit it is slightly larger than the carbonyl shift in peroxyformic acid. The photoelectron spectrum of peroxyformate ion produced from the reaction of HOO^- with ethyl formate, identifies ν_4 (1098 ± 20 cm^{-1}), ν_5 (973 ± 20 cm^{-1}), and ν_6 (574 ± 35 cm^{-1}) for the formylperoxy radical.[22]

In the computation of the *cis*-$\tilde{X}\,^2A''$ C=O stretching frequency, a potential Fermi resonance with the C−O′ stretch had to be considered. A standard procedure, provided by Nielson,[59] modifies the VPT2 treatment, in instances when $\nu_r \approx \nu_s + \nu_t$, by computing a replacement term for the anharmonic constant x_{rs} (see supporting information). In this work, the Nielson correction for the Fermi resonance altered the VPT2 anharmonic correction by up to 27 cm^{-1} [for the *cis*-HC(^{18}O)OO isotopologue].

3.4 Isotopologues

The equilibrium internuclear distances (r_e) and vibrationally averaged equilibrium parameters ($r_{g,0K}$), at 0 K, for both the states and conformers of the parent molecule and the five ground state isotopologues are reported in Table 7. According to the following method, each distance is expanded in the leading terms of its normal coordinate Taylor expansion and averaged with respect to the ground vibrational state[51,60,61]

$$r_{g,0K} = \langle r\rangle_{g,0K} \approx r_e + \sum_s \left(\frac{\partial r}{\partial Q_s}\right)_e \langle Q_s\rangle_{0K} + \frac{1}{2}\sum_s \left(\frac{\partial^2 r}{\partial Q_s^2}\right)_e \langle Q_s^2\rangle_{0K} \quad (4)$$

In Equation 4, $\langle Q_s\rangle$, the linear term, is averaged with respect to the VPT2 anharmonic vibrational wave function, and $\langle Q_s^2\rangle$, the quadratic term, is averaged with respect to the harmonic vibrational wave function. The equilibrium geometries were obtained with the CCSD(T)/ANO2 method and vibrational corrections predicted at CCSD(T)/ANO1. These vibrationally-averaged internuclear separations experience increases as great as 0.02 Å from the equilibrium distance, in the case of the C−H bond length. The increase is not unexpected, as the modes of the C–H bond are associated with the highest degree of anharmonicity in the system (with $\delta\nu_1 = 150$ cm^{-1}).

Tables 8 and 9 show the VPT2-corrected CCSD(T)/ANO2 vibrational frequencies for various isotopologues of the $\tilde{X}\,^2A''$-*cis* and $\tilde{X}\,^2A''$-*trans* formylperoxy radical. Isotopic frequency shifts from the parent isomer are presented in Table 10.

3.4.1 H^{13}C(O)OO

Carbon-13 substitution causes a 2-3% red-shift relative to parent frequencies for any modes involving this atom. Specifically, the C=O stretch shifts by −39 cm^{-1}, the C–O′ stretch by −26 cm^{-1}, and the C–H stretch by −13 cm^{-1} in the *trans* isotopomer. For the *cis* isotopomer, the shifts from the parent are −40 cm^{-1}, −24 cm^{-1}, and −12 cm^{-1}, respectively. The wag motion decreases

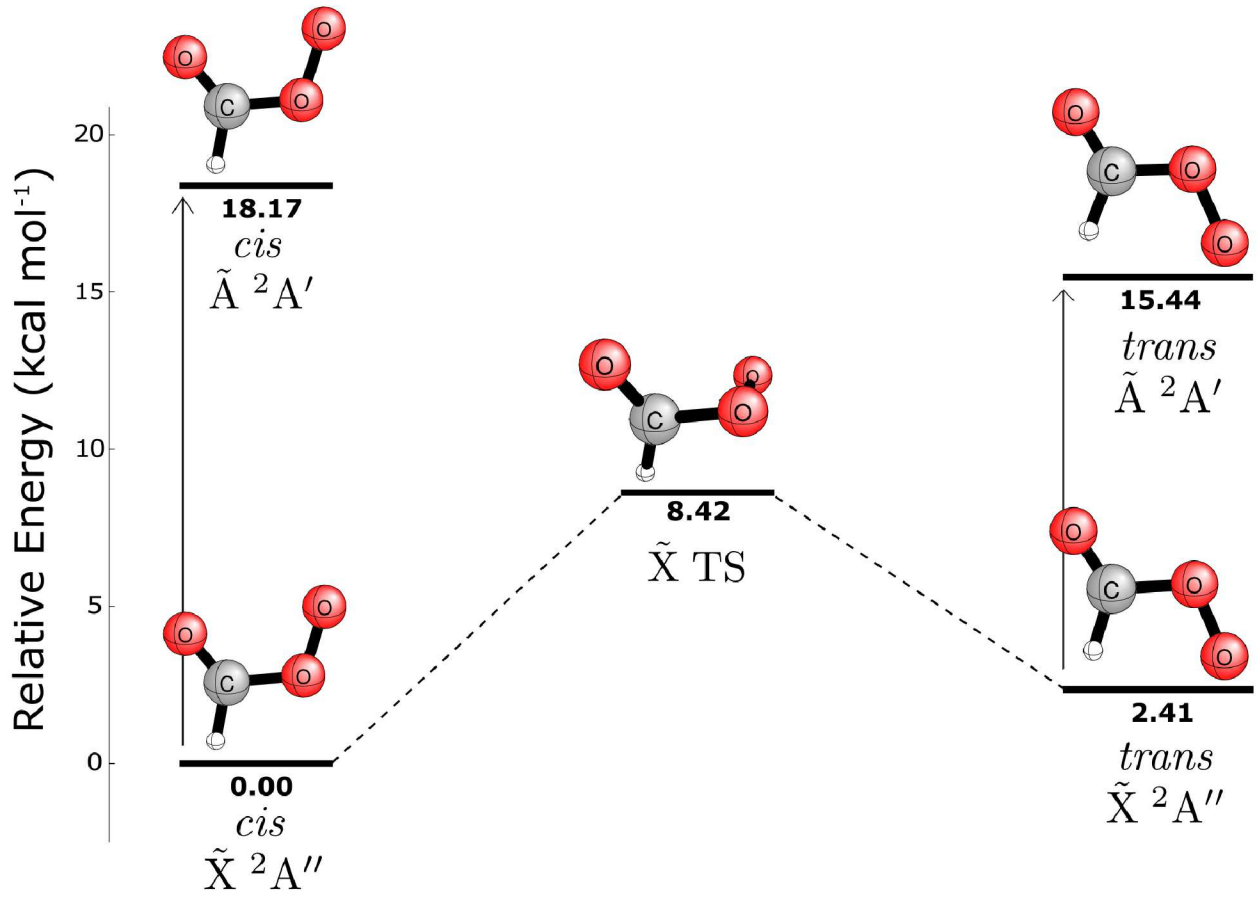

Fig. 3 Potential energy diagram for formylperoxy radical including core, relativistic, DBOC, and ZPVE corrections (in kcal mol^{-1}). The electronic energies are extrapolated to the CBS limit.

by twice as much from ^{13}C substitution in the *trans* isomer (−27 cm^{-1} from its parent), than in the *cis* (−13 cm^{-1} from its parent).

3.4.2 HC(^{18}O)OO

The frequencies of the *cis* and *trans* conformers respond differently to ^{18}O substitution of the carbonyl group. For example, the *cis* isotopomer shows an 81 cm^{-1} decrease in the C=O stretching frequency, whereas the *trans* isotopomer shows only a 39 cm^{-1} decrease. This substitution, however, causes a much smaller shift in the *cis* (1 cm^{-1} decrease) than in the *trans* conformer (17 cm^{-1} decrease) for the C–O′ stretch. From these two stretches, the *cis* isomer appears to localize the effects of the mass change to directly interacting modes of the substituted atom, whereas the *trans* isomer experiences smaller change in those modes. The mass change effects, rather, are spread out across the system. Such dispersion across the *trans* system supports the conclusion that the lower energy of the *trans* conformer may be attributed to greater hyperconjugation effects in its system than in the *cis*.

3.4.3 HC(O)^{18}O^{18}O

Substitution of both peroxy oxygens with ^{18}O diminishes the frequencies of modes involving these atoms by 1-5%. Most significantly, the O′–O″ stretch of both conformers decreases by 58 cm^{-1}. The C–O′ stretch decreases by 32 cm^{-1} in the *trans* conformer and, contrastingly, by 10 cm^{-1} in the *cis*. The *cis* structure, however, experiences a greater shift to the O=C–O′ bend due to the peroxy substitution than does the *trans*, with −31 cm^{-1} and −13 cm^{-1} shifts, respectively. This mode, in the *cis* conformer, may expose atoms O and O′ to more repulsive effects that are not present in the *trans* structure, making the *trans* structure the more malleable of the conformers for the O=C–O′ bend frequency.

3.4.4 DC(O)OO

H→D substitution induces the largest shifts, since it effects the largest relative change in nuclear mass. For the *trans* species, substitution to DC(O)OO greatly diminishes the C–H stretch and HCO bend modes (by 700 cm^{-1} and 301 cm^{-1}, respectively). The *cis* conformer experiences even greater frequency shifts as a result of the deuterium substitution, with isotopic shifts of 709 cm^{-1} (ν_1, C–D stretch) and 343 cm^{-1} (ν_3, DCO bend). Shifts for both species arise in the out-of-plane wag motion as well. The ν_8 wag mode has a 158 cm^{-1} decrease for the *trans* and 147 cm^{-1} for the *cis*. A previous theoretical study on the methylperoxy radical noted the same decrease of >20% in the magnitude of fundamental frequencies upon deuteration.[62] For DC(O)OO, even the C=O stretch is affected, showing a 40 cm^{-1} redshift. Here we see the significance of the hydrogen mass increase – it causes a greater impact on the C=O stretch than does changing the mass

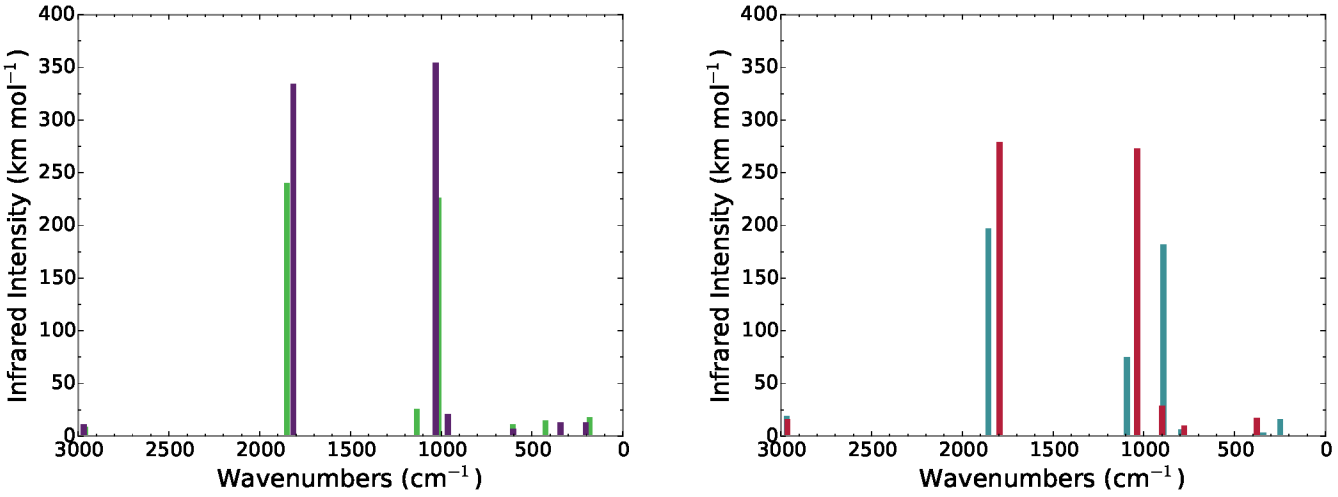

Fig. 4 Infrared vibrational spectra of $\tilde{X}\,^2A''$ *trans*-HC(O)OO (green), $\tilde{A}\,^2A'$ *trans*-HC(O)OO (purple), $\tilde{X}\,^2A''$ *cis*-HC(O)OO (blue), and $\tilde{A}\,^2A'$ *cis*-HC(O)OO (red).

of either the participating oxygen or carbon atoms. The IR intensities experience a large impact from deuterium substitution as well. Whereas the HCO bend IR intensities are extremely small ($\leq$1 km mol^{-1}), the DCO bend is surprisingly intense (165 km mol^{-1}).

3.4.5 DC(O)^{18}O^{18}O

H$\rightarrow$D in conjunction with O′O″$\rightarrow^{18}$O′^{18}O″ substitution evokes similar changes to the frequencies as the deuterium substitution does by itself. For the *trans* species, the DC(O)^{18}O^{18}O frequencies shift from HC(O)OO by 700 cm^{-1} (ν_1, C–D stretch), 304 cm^{-1} (ν_3, DCO bend), and 159 cm^{-1} (ν_8, wag). The frequencies of *cis* conformer decrease after substitution with these three isotopes by 701 cm^{-1} (ν_1, C–D stretch), 347 cm^{-1} (ν_3, DCO bend), and 149 cm^{-1} (ν_8, wag). These are all within 3 cm^{-1} of the shifts due solely to deuterium substitution (DC(O)OO). The DC(O)^{18}O^{18}O shifts vary from DC(O)OO, as expected, most significantly for the O′–O″ stretch ($-$60 cm^{-1} in *trans* and $-$26 cm^{-1} in *cis*), which is more closely aligned to the HC(O)^{18}O^{18}O shifts.

Many of these isotopic substitutions have been achieved in experiment to aid both mode and isomer identification in the spectroscopic studies.[21,56] While Tso and Lee did not find an O′–O″ stretch for the parent isotopomer, they assigned the O′–O″ fundamental for DC(O)OO$^\bullet$ (ν_4, 1143.4 cm^{-1}) and DC(O)^{18}O^{18}O$^\bullet$ (ν_4, 1125.6 cm^{-1}).[56] We report the stretches for DC(O)OO$^\bullet$ (ν_4, 1123 cm^{-1}) and DC(O)^{18}O^{18}O$^\bullet$ (ν_4, 1064 cm^{-1}). Though the agreement is poor, it should be noted that the experimental fundamentals of Tso and Lee[10] differed from gas phase measurements of Lineberger and coworkers[22] by 100 cm^{-1} on their only mutually assigned frequency, the ν_5 mode.

Table 11 compares the isotopic vibrational frequency shifts to experimental findings,[21,63] for the two highest IR intensity modes (ν_2, C=O stretch and ν_5, C–O′ stretch). For each isotopic substitution of the *trans* isomer, which is the only experimentally reported conformer, the computed shift from the parent vibrational frequency for the C=O stretch is within 4 cm^{-1} from the isotopic shift collected in the Ar matrix. For the C–O′ stretch, the computed shift from the frequencies of the parent isotopologue for each isotopic substitution is found to be 7-13 cm^{-1} larger than those measured in the Ar matrix. Though this deviation from experiment is large in contrast to the precision of the C=O stretch, it falls within the bounds of Ar matrix standard deviation (which affords uncertainty of 9 cm^{-1} for the parent C–O′ stretch and $\approx$8 cm^{-1} for that of the isotologues).[58]

4 Conclusions

Experimental studies of the formylperoxy radical still leave many important questions unanswered.[10,15,16,21,22,56,63] The only experimental fundamentals are those for the *trans*-$\tilde{X}\,^2A''$ electronic state. There are no experimental fundamentals for the *trans*-$\tilde{A}\,^2A'$, *cis*-$\tilde{X}\,^2A''$, or *cis*-$\tilde{A}\,^2A'$ structures. In fact, there is no experimental information concerning the *cis* $\tilde{X}$ and $\tilde{A}$ states at all. The only experimental result for the *trans*-$\tilde{A}\,^2A'$ state is its $\tilde{X}\rightarrow\tilde{A}$ excitation energy, determined from a single peak in the photoelectron spectrum by Lineberger and coworkers.[22]

In this research, stationary points on the ground ($\tilde{X}$) and first excited ($\tilde{A}$) electronic state surfaces of the formylperoxy radical have been examined using coupled-cluster methods. On the $\tilde{X}$ surface, we find two minimum energy conformers connected by internal rotation of the terminal peroxy, designated *cis* and *trans*. These conformers are predicted to be separated by 2.41 kcal mol^{-1} with *trans* being lower in energy, and the isomerization barrier lies 8.42 kcal mol^{-1} above the *trans* in energy. Adiabatic electronic transitions to the excited state ($\tilde{A}\leftarrow\tilde{X}$) for the *cis* and *trans* conformers are predicted to be 13.03 kcal mol^{-1} and 18.17 kcal mol^{-1}, respectively. Our theoretical excitation energy is in excellent agreement with the experimental value of 18.1 $\pm$ 1.4 kcal mol^{-1} of Lineberger and coworkers.[22] Upon electronic excitation, the O′O″ bond length increases as expected for peroxy species. The energetic ordering of the *cis* and *trans* conformers is reversed in the $\tilde{A}\,^2A'$ excited state, possibly due to the long-range intramolecular interaction between terminal oxygen

Table 5 Vibrational frequencies (cm^{-1}) and IR intensities (km mol^{-1}) for the *trans* isomer with harmonic frequencies (ω), anharmonic corrections ($\delta\nu$), and Brueckner corrections ($\delta\omega$).

		trans					*cis*				
Mode	Description	ω^a	$\delta\nu^b$	$\delta\omega^c$	ν^d	Intensity^e	ω^a	$\delta\nu^b$	$\delta\omega^c$	ν^d	Intensity^e
$\tilde{X}\,^2A''$											
$\nu_1(a')$	CH str	3099	−152	−1	2946	9	3107	−153	−1	2953	19
$\nu_2(a')$	CO str	1866	−31	0	1835	240	1860	−18	0	1842	197
$\nu_3(a')$	HCO bend	1333	−35	−1	1296	1	1373	−34	−1	1338	1
$\nu_4(a')$	O′O″ str	1144	−20	−5	1119	26	1109	−28	−2	1079	75
$\nu_5(a')$	CO′ str	1016	−15	−1	1000	226	906	−27	−2	877	182
$\nu_6(a')$	OCO′ bend	604	−13	−1	590	11	800	−18	−1	780	6
$\nu_7(a')$	CO′O″ bend	414	−3	−1	410	15	335	−7	0	328	3
$\nu_8(a'')$	wag	1014	−22	0	991	<1	986	−28	−1	957	<1
$\nu_9(a'')$	torsion	171	−4	0	167	18	238	−6	0	233	16
$\tilde{A}\,^2A'$											
$\nu_1(a')$	CH str	3108	−153	0	2955	11	3108	−158	−1	2949	16
$\nu_2(a')$	CO str	1833	−33	0	1800	334	1815	−35	1	1780	279
$\nu_3(a')$	HCO bend	1395	−33	−2	1360	1	1380	−41	−1	1337	1
$\nu_4(a')$	O′O″ str	957	−1	−7	949	21	895	−6	−5	884	29
$\nu_5(a')$	CO′ str	1054	−35	−4	1015	354	1063	−36	−6	1021	273
$\nu_6(a')$	OCO′ bend	599	−8	−2	589	7	773	−9	−2	762	10
$\nu_7(a')$	CO′O″ bend	333	−5	0	328	13	255	−3	−1	251	1
$\nu_8(a'')$	wag	1008	−19	−1	988	<1	1012	−23	−1	989	1
$\nu_9(a'')$	torsion	192	−3	0	189	13	375	−12	0	363	17

[a] Computed with CCSD(T)/ANO2.
[b] Computed with CCSD(T)/ANO1.
[c] BCCSD(T)/ANO1 − UHF-CCSD(T)/ANO1 harmonic vibrational frequencies.
[d] $\omega + \delta\nu + \delta\omega$.
[e] CCSD(T)/ANO2 harmonic IR intensities.

Table 6 Summary of previous and present research on the vibrational frequencies of the *trans* and *cis* conformations of the formylperoxy radical.

Method	$\nu_1(a')$	$\nu_2(a')$	$\nu_3(a')$	$\nu_4(a')$	$\nu_5(a')$	$\nu_6(a')$	$\nu_7(a')$	$\nu_8(a'')$	$\nu_9(a'')$
FTIR in O_2 matrix (*trans*)[a]		1788/1787			1091				
FTIR in Ar matrix (*trans*)[b]		1822			957				
Gas Phase Experiments (*trans*)[c]				1078 ± 20	966 ± 20	574 ± 35			
CCSD(T)/ANO2 (*trans*-$\tilde{X}\,^2A''$)[d]	2946	1835	1296	1119	1000	590	410	991	167
CCSD(T)/ANO2 (*cis*-$\tilde{X}\,^2A''$)[d]	2953	1842	1338	1079	877	780	328	957	233
CCSD(T)/ANO2 (*trans*-$\tilde{A}\,^2A'$)[d]	2955	1800	1360	949	1015	589	328	988	189
CCSD(T)/ANO2 (*cis*-$\tilde{A}\,^2A'$)[d]	2949	1780	1337	884	1021	762	251	989	363

[a] Tso and Lee (Ref. 56.)
[b] Yang et al. (Ref. 21).
[c] Lineberger and coworkers (Ref. 22).
[d] Anharmonic corrected frequencies found in this work.

atoms. We predict lifetimes of $\tau_{\tilde{A}} \approx 5.4$ ms and $\tau_{\tilde{A}} \approx 20.5$ ms for the *trans* and *cis* electronic excited states, respectively. To aid in spectral characterization, we also predict the anharmonic vibrational frequencies of the two ground state minima and find agreement within the expected bounds of Ar matrix experiments and outside the error bounds of gas-phase ν_4 and ν_5 modes by 20 cm^{-1}. We provide rigorous predictions for the four modes lacking experimental assignment. Frequency analyses for $H^{13}C(O)OO^{\bullet}$, $HC(^{18}O)OO^{\bullet}$, $HC(O)^{18}O^{18}O^{\bullet}$, $DC(O)OO^{\bullet}$, and $DC(O)^{18}O^{18}O^{\bullet}$ isotopologues show excellent agreement with experimental values.

5 Acknowledgement

This research was supported by the Department of Energy, Basic Energy Sciences, Division of Chemical Sciences, Fundamental Interactions Team, Grant No. DEFG02-97-ER14748. We thank Dr. Jay Agarwal and Andreas V. Copan for helpful discussions.

References

1 D. J. Dixon and G. Skirrow, *The Gas Phase Combustion of Aldehydes*, Elsevier, Amsterdam, 1977, vol. 17, pp. 369 – 439.
2 T. Takeno, *Turbulence and Molecular Processes in Combustion*, Elsevier Science, 2012.
3 B. Finlayson-Pitts and J. Pitts, *Chemistry of the Upper and Lower Atmosphere: Theory, Experiments, and Applications*, Elsevier Science, 1999.
4 J. A. Miller, R. J. Kee and C. K. Westbrook, *Annu. Rev. Phys. Chem.*, 1990, **41**, 345–387.
5 R. T. Pollard, *Hydrocarbons*, Elsevier, Amsterdam, 1977, vol. 17, pp. 249–367.
6 B. J. Finlayson and J. N. J. Pitts, *Science*, 1976, **192**, 111–119.
7 H. Okabe, *Photochemistry of Small Molecules*, Wiley, New York, 1978.
8 T. L. Osif and J. Heicklen, *J. Phys. Chem.*, 1976, **80**, 1526–1531.

Table 7 Equilibrium bond lengths (r_e) optimized at CCSD(T)/ANO2 and vibrationally averaged ($r_{g,0K}$) computed at CCSD(T)/ANO1 in Ångstrom for both the *trans*- and *cis*-$\tilde{X}\,^2A''$ formylperoxy radicals and five of their isotopologues along with the $\tilde{A}\,^2A'$ formylperoxy parent radicals.

	$HC(O)O_2$	$HC(O)O_2$	$DC(O)O_2$	$H^{13}C(O)O_2$	$HC(^{18}O)O_2$	$HC(O)^{18}O_2$	$DC(O)^{18}O_2$	$HC(O)O_2$	$HC(O)O_2$
	r_e	$r_{g,0K}$						r_e	$r_{g,0K}$
				trans-$\tilde{X}\,^2A''$				*trans*-$\tilde{A}\,^2A'$	
r(C–H)	1.0943	1.1157	1.1099	1.1157	1.1157	1.1157	1.1100	1.0920	1.1132
r(C=O)	1.1920	1.1967	1.1967	1.1966	1.1965	1.1967	1.1967	1.1873	1.1919
r(C–O′)	1.4166	1.4286	1.4281	1.4284	1.4286	1.4284	1.4278	1.3841	1.3942
r(O′–O″)	1.3297	1.3358	1.3359	1.3358	1.3358	1.3354	1.3356	1.3862	1.3932
				cis-$\tilde{X}\,^2A''$				*cis*-$\tilde{A}\,^2A'$	
r(C–H)	1.0932	1.1146	1.1089	1.1146	1.1146	1.1146	1.1089	1.0930	1.1145
r(C=O)	1.1816	1.1863	1.1863	1.1862	1.1863	1.1861	1.1863	1.1895	1.1941
r(C–O′)	1.4162	1.4276	1.4271	1.4274	1.4273	1.4276	1.4269	1.3709	1.3810
r(O′–O″)	1.3283	1.3351	1.3351	1.3351	1.3347	1.3351	1.3347	1.3837	1.3918

Table 8 Vibrational frequencies (cm^{-1}) and IR intensities (km mol^{-1}) of various isotopologues of the $^2A''$ *cis* formylperoxy radical. Harmonic frequencies (ω), anharmonic corrections ($\delta\nu$), and fundamentals (ν) are reported.[a]

Mode	Description	ω	$\delta\nu$	ν	Intensity
$H^{13}C(O)OO$					
$\nu_1(a')$	CH str	3096	−154	2942	17
$\nu_2(a')$	CO str	1819	−17	1802	185
$\nu_3(a')$	HCO bend	1371	−34	1337	0
$\nu_4(a')$	O′O″ str	1108	−28	1080	68
$\nu_5(a')$	CO′ str	883	−27	855	180
$\nu_6(a')$	OCO′ bend	796	−18	779	5
$\nu_7(a')$	CO′O″ bend	335	−7	328	3
$\nu_8(a'')$	wag	972	−28	945	0
$\nu_9(a'')$	torsion	236	−6	230	15
$HC(O)^{18}O^{18}O$					
$\nu_1(a')$	CH str	3107	−154	2953	19
$\nu_2(a')$	CO str	1860	−23	1837	198
$\nu_3(a')$	HCO bend	1370	−33	1338	1
$\nu_4(a')$	O′O″ str	1049	−26	1023	78
$\nu_5(a')$	CO′ str	894	−25	869	166
$\nu_6(a')$	OCO′ bend	768	−18	750	8
$\nu_7(a')$	CO′O″ bend	324	−7	318	2
$\nu_8(a'')$	wag	985	−40	945	0
$\nu_9(a'')$	torsion	232	−5	227	16
$HC(^{18}O)OO$					
$\nu_1(a')$	CH str	3107	−161	2946	19
$\nu_2(a')$	CO str	1818	−58	1761	193
$\nu_3(a')$	HCO bend	1369	−33	1335	0
$\nu_4(a')$	O′O″ str	1109	−29	1080	74
$\nu_5(a')$	CO′ str	905	−27	878	182
$\nu_6(a')$	OCO′ bend	790	−18	772	5
$\nu_7(a')$	CO′O″ bend	327	−7	320	2
$\nu_8(a'')$	wag	984	−29	955	0
$\nu_9(a'')$	torsion	237	−6	231	15
DC(O)OO					
$\nu_1(a')$	CH str	2324	-79	2245	35
$\nu_2(a')$	CO str	1813	−32	1781	191
$\nu_3(a')$	HCO bend	1032	−36	996	100
$\nu_4(a')$	O′O″ str	1128	−28	1100	32
$\nu_5(a')$	CO′ str	851	−22	830	113
$\nu_6(a')$	OCO′ bend	794	−18	776	6
$\nu_7(a')$	CO′O″ bend	334	−7	327	3
$\nu_8(a'')$	wag	826	−15	810	2
$\nu_9(a'')$	torsion	215	−5	211	9
$DC(O)^{18}O^{18}O$					
$\nu_1(a')$	CH str	2324	−79	2245	35
$\nu_2(a')$	CO str	1812	−31	1781	191
$\nu_3(a')$	HCO bend	1020	−26	994	120
$\nu_4(a')$	O′O″ str	1076	−21	1055	8
$\nu_5(a')$	CO′ str	840	−20	820	105
$\nu_6(a')$	OCO′ bend	763	−17	746	9
$\nu_7(a')$	CO′O″ bend	323	−6	317	2
$\nu_8(a')$	wag	825	−16	809	2
$\nu_9(a')$	torsion	209	−4	205	10

[a] See Table 5 and Theoretical Methods for abbreviations and details.

9 H. E. Radford, K. M. Evenson and C. J. Howard, *J. Chem. Phys.*, 1974, **60**, 3178–3183.

10 T. L. Tso, M. Diem and E. K. C. Lee, *Chem. Phys. Lett.*, 1982, **91**, 339–342.

11 J. S. Francisco and I. H. Willams, *J. Phys. Chem.*, 1988, **92**, 5347–5352.

12 A. O. Langford and C. B. Moore, *J. Chem. Phys.*, 1984, **80**, 4211–4221.

13 C. C. Hsu, A. M. Mebel and M. C. Lin, *J. Chem. Phys.*, 1996, **105**, 2346–2352.

14 T. L. Allen, W. H. Fink and D. H. Volman, *J. Photochem. Photobiol. A*, 1995, **85**, 201–205.

15 H.-C. Yang, H.-L. Chen and J.-J. Ho, *J. Mol. Struct.*, 2006, **774**, 35–41.

16 A. A. Nickel, J. G. Lanorio and K. M. Ervin, *J. Phys. Chem. A*, 2013, **117**, 1021–1029.

17 T. L. Allen, W. H. Fink and D. H. Volman, *J. Phys. Chem.*, 1996, **100**, 5299–5302.

18 D. H. Volman, *J. Photochem. Photobiol. A*, 1996, **100**, 1–3.

19 J. Zádor, C. A. Taatjes and R. X. Fernandes, *Prog. Energy Combust. Sci.*, 2011, **37**, 371–421.

20 N. W. Winter and W. A. Goddard, *Chem. Phys. Lett.*, 1975, **33**, 25–29.

21 R. Yang, L. Yu, A. Zeng and M. Zhou, *J. Phys. Chem. A*, 2004, **108**, 4228–4231.

22 S. M. Villano, N. Eyet, S. W. Wren, G. B. Ellison, V. M. Bierbaum and W. C. Lineberger, *J. Phys. Chem. A*, 2010, **114**, 191–200.

23 J. J. Orlando and G. S. Tyndall, *Chem. Soc. Rev.*, 2012, **41**, 6294–6317.

24 CFOUR, a quantum chemical program package written by J.F. Stanton, J. Gauss, J.D. Watts, P.G. Szalay, R.J. Bartlett with contributions from A.A. Auer, D.E. Bernholdt, O.Christiansen, M.E. Harding, M. Heckert, O. Heun, C. Huber, D. Jonsson, J. Jusélius, W.J. Lauderdale, T. Metzroth, C. Michauk, D.P. O'Neill, D.R. Price, K. Ruud, F. Schiff-

Table 9 Vibrational frequencies (cm^{-1}) and IR intensities (km mol^{-1}) of various isotopologues of the $^2A''$ *trans* formylperoxy radical. Harmonic frequencies (ω), anharmonic corrections ($\delta\nu$), and fundamentals (ν) are reported.[a]

Mode	Description	ω	$\delta\nu$	ν	Intensity
$H^{13}C(O)OO$					
$\nu_1(a')$	CH str	3088	−155	2934	9
$\nu_2(a')$	CO str	1826	−29	1796	224
$\nu_3(a')$	HCO bend	1332	−34	1297	1
$\nu_4(a')$	O′O″ str	1143	−21	1122	28
$\nu_5(a')$	CO′ str	994	−20	974	214
$\nu_6(a')$	OCO′ bend	600	−12	588	11
$\nu_7(a')$	CO′O″ bend	412	−4	408	15
$\nu_8(a'')$	wag	1000	−36	964	0
$\nu_9(a'')$	torsion	170	−3	166	17
$HC(O)^{18}O^{18}O$					
$\nu_1(a')$	CH str	3099	−149	2950	9
$\nu_2(a')$	CO str	1866	−32	1834	242
$\nu_3(a')$	HCO bend	1331	−33	1298	1
$\nu_4(a')$	O′O″ str	1083	−16	1067	23
$\nu_5(a')$	CO′ str	992	−24	968	218
$\nu_6(a')$	OCO′ bend	589	−11	578	11
$\nu_7(a')$	CO′O″ bend	399	−1	398	14
$\nu_8(a'')$	wag	1012	−22	990	0
$\nu_9(a'')$	torsion	167	−4	163	19
$HC(^{18}O)OO$					
$\nu_1(a')$	CH str	3099	−158	2941	9
$\nu_2(a')$	CO str	1825	−29	1796	234
$\nu_3(a')$	HCO bend	1329	−32	1297	1
$\nu_4(a')$	O′O″ str	1144	−19	1125	26
$\nu_5(a')$	CO′ str	1015	−31	984	225
$\nu_6(a')$	OCO′ bend	590	−11	579	10
$\nu_7(a')$	CO′O″ bend	410	−2	408	15
$\nu_8(a'')$	wag	1012	−22	990	0
$\nu_9(a'')$	torsion	169	−4	165	18
DC(O)OO					
$\nu_1(a')$	CH str	2323	−75	2247	24
$\nu_2(a')$	CO str	1815	−27	1788	235
$\nu_3(a')$	HCO bend	1011	−15	996	165
$\nu_4(a')$	O′O″ str	1143	−20	1123	27
$\nu_5(a')$	CO′ str	980	−19	961	48
$\nu_6(a')$	OCO′ bend	600	−11	589	10
$\nu_7(a')$	CO′O″ bend	402	−4	398	14
$\nu_8(a'')$	wag	848	−14	833	2
$\nu_9(a'')$	torsion	162	−4	158	13
$DC(O)^{18}O^{18}O$					
$\nu_1(a')$	CH str	2322	−75	2247	24
$\nu_2(a')$	CO str	1815	−28	1787	237
$\nu_3(a')$	HCO bend	1004	−10	994	103
$\nu_4(a')$	O′O″ str	1081	−17	1064	22
$\nu_5(a')$	CO′ str	960	−22	938	104
$\nu_6(a')$	OCO′ bend	585	−11	574	10
$\nu_7(a')$	CO′O″ bend	388	−4	384	13
$\nu_8(a'')$	wag	846	−14	832	2
$\nu_9(a'')$	torsion	158	−3	154	13

[a] See Table 5 and Theoretical Methods for additional information.

mann, A. Tajti, M.E. Varner, J. Vázquez and the integral packages: MOLECULE (J. Almlöf and P.R. Taylor), PROPS (P.R. Taylor), ABACUS (T. Helgaker, H.J. Aa. Jensen, P. Jørgensen, and J. Olsen), and ECP routines by A.V. Mitin and C. van Wüllen. For the current version see, http://www.cfour.de.

25 M. E. Harding, T. Metzroth, J. Gauss and A. A. Auer, *J. Chem. Theory Comput.*, 2008, **4**, 64–74.

26 M. Kállay and J. Gauss, *J. Chem. Phys.*, 2005, **123**, 214105.

27 J. M. Turney, A. C. Simmonett, R. M. Parrish, E. G. Hohenstein, F. A. Evangelista, J. T. Fermann, B. J. Mintz, L. A. Burns, J. J. Wilke, M. L. Abrams, N. J. Russ, M. L. Leininger, C. L. Janssen, E. T. Seidl, W. D. Allen, H. F. Schaefer, R. A. King, E. F. Valeev, C. D. Sherrill and T. D. Crawford, *WIREs: Comput. Mol. Sci.*, 2011, **2**, 556–565.

28 T. H. Dunning, *J. Chem. Phys.*, 1989, **90**, 1007–1023.

29 J. Almlöf and P. R. Taylor, *J. Chem. Phys.*, 1987, **86**, 4070–4077.

30 L. McCaslin and J. Stanton, *Mol. Phys.*, 2013, **111**, 1492–1496.

31 P. G. Szalay, J. Gauss and J. F. Stanton, *Theor. Chem. Acc.*, 1998, **100**, 5–11.

32 T. J. Lee and P. R. Taylor, *Int. J. Quant. Chem.*, 1989, **36**, 199–207.

33 D. Jayatilaka and T. J. Lee, *J. Chem. Phys.*, 1993, **98**, 9734–9747.

34 J. D. Watts, M. Urban and R. J. Bartlett, *Theor. Chem. Acc.*, 1995, **90**, 341–355.

35 A. V. Copan, A. E. Wiens, E. M. Nowara, H. F. Schaefer and J. Agarwal, *J. Chem. Phys.*, 2015, **142**, 055303.

36 A. L. L. East and W. D. Allen, *J. Chem. Phys.*, 1993, **99**, 4638–4650.

37 A. G. Császár, W. D. Allen and H. F. Schaefer, *J. Chem. Phys.*, 1998, **108**, 9751–9764.

38 J. M. Gonzales, C. Pak, R. S. Cox, W. D. Allen, H. F. Schaefer, A. G. Császár and G. Tarczay, *Chem. Eur. J.*, 2003, **9**, 2173–2192.

39 N. L. Allinger, J. T. Fermann, W. D. Allen and H. F. Schaefer, *J. Chem. Phys.*, 1997, **106**, 5143–5150.

40 Y. J. Bomble, J. F. Stanton, M. Kállay and J. Gauss, *J. Chem. Phys.*, 2005, **123**, 054101.

41 M. Kállay and J. Gauss, *J. Chem. Phys.*, 2008, **129**, 144101.

42 R. D. Cówan and D. C. Griffin, *J. Opt. Soc. Am.*, 1976, **66**, 1010–1014.

43 W. Kutzelnigg and E. Ottschofski, *J. Chem. Phys.*, 1995, **102**, 1752–1757.

44 E. R. Davidson, Y. Ishikawa and G. L. Malli, *Chem. Phys. Lett.*, 1981, **84**, 226–227.

45 C. W. Bauschlicher, J. M. L. Martin and P. R. Taylor, *J. Phys. Chem. A*, 1999, **103**, 7715–7718.

46 H. Sellers and P. Pulay, *Chem. Phys. Lett.*, 1984, **103**, 463–465.

47 N. C. Handy, Y. Yamaguchi and H. F. Schaefer, *J. Chem. Phys.*, 1986, **84**, 4481–4484.

48 R. A. Chiles and C. E. Dykstra, *J. Chem. Phys.*, 1981, **74**, 4544–4556.

49 J. F. Stanton, J. Gauss and R. J. Bartlett, *J. Chem. Phys.*, 1992, **97**, 5554–5559.

50 I. S. Ignatyev, Y. Xie, W. D. Allen and H. F. Schaefer, *J. Chem. Phys.*, 1997, **107**, 141–155.

51 A. V. Copan, H. F. Schaefer and J. Agarwal, *Mol. Phys.*, 2015.

52 A. Li, D. Xie, R. Dawes, A. W. Jasper, J. Ma and H. Guo, *J. Chem. Phys.*, 2010, **133**, 144306.

53 R. Tuckett, P. Freedman and W. Jones, *Mol. Phys.*, 1979, **37**, 403–408.

Table 10 Isotopic shifts (cm^{-1}) for the $^2A''$ *trans* and *cis* formylperoxy radicals. Predicted results are from CCSD(T)/ANO1 VPT2-corrected CCSD(T)ANO2 frequencies.

	HC(O)OO	$H^{13}C(O)OO$	$HC(^{18}O)OO$	$HC(O)^{18}O^{18}O$	DC(O)OO	$DC(O)^{18}O^{18}O$
trans						
$\nu_1(a')$	0	−13	−6	+3	−700	−700
$\nu_2(a')$	0	−39	−39	−1	−47	−48
$\nu_3(a')$	0	0	0	0	−301	−304
$\nu_4(a')$	0	−2	+1	−58	−1	−60
$\nu_5(a')$	0	−26	−17	−32	−40	−62
$\nu_6(a')$	0	−3	−12	−13	−2	−17
$\nu_7(a')$	0	−2	−2	−13	−13	−27
$\nu_8(a'')$	0	−27	−2	−1	−158	−159
$\nu_9(a'')$	0	−1	−2	−4	−9	−13
cis						
$\nu_1(a')$	0	−12	−8	−1	−709	−709
$\nu_2(a')$	0	−40	−81	−5	−61	−61
$\nu_3(a')$	0	−2	−4	−2	−343	−346
$\nu_4(a')$	0	−1	−1	−58	+20	−26
$\nu_5(a')$	0	−24	−1	−10	−49	−59
$\nu_6(a')$	0	−3	−9	−31	−5	−36
$\nu_7(a')$	0	0	−8	−10	−1	−11
$\nu_8(a'')$	0	−13	−3	−13	−147	−149
$\nu_9(a'')$	0	−2	−1	−5	−22	−27

Table 11 Summary of previous and current research on isotopic frequency shift (cm^{-1}) with respect to HC(O)OO.

	$H^{13}C(O)OO$	$HC(^{18}O)OO$	$HC(O)^{18}O^{18}O$	DC(O)OO	$DC(O)^{18}O^{18}O$
C=O stretch					
Matrix-isolated in O_2-*trans*[a]	−40	−69	−1	−31	−32
FTIR in solid Ar-*trans*[b]	−38	−39	−5	−46	
CCSD(T)/ANO2-*trans*[c]	−39	−39	−1	−47	−48
CCSD(T)/ANO2-*cis*[c]	−40	−81	−5	−61	−61
C–O stretch					
Matrix-isolated in O_2-*trans*[a]	−22	−1	−22		
FTIR in solid Ar-*trans*[b]	−19	−4	−24		
CCSD(T)/ANO2-*trans*[c]	−26	−17	−32	−40	−62
CCSD(T)/ANO2-*cis*[c]	−24	−1	−10	−49	−59

[a] Tso et al. (Ref. 63).
[b] Yang et al. (Ref. 21).
[c] Anharmonic corrected shift found in this work.

54 M. S. Schuurman, S. R. Muir, W. D. Allen and H. F. Schaefer, *J. Chem. Phys.*, 2004, **120**, 11586–11599.

55 S. J. Strickler and R. A. Berg, *J. Chem. Phys.*, 1962, **37**, 814–822.

56 T. L. Tso and E. K. C. Lee, *J. Phys. Chem.*, 1984, **88**, 5465–5474.

57 M. E. Jacox, *Chem. Phys.*, 1994, **189**, 149–170.

58 M. E. Jacox, *Chem. Soc. Rev.*, 2002, **31**, 108–115.

59 H. H. Nielsen, *Rev. Mod. Phys.*, 1951, **23**, 90–136.

60 A. G. Császár, *Equilibrium Molecular Structure: From Spectroscopy to Quantum Chemistry*, CRC Press, Boca Raton, FL, 2011, pp. 233–262.

61 K. Kuchitsu, *Accurate Molecular Structures: Their Determination and Importance*, Oxford University Press, Oxford, UK, 1992, pp. 14–43.

62 J. Agarwal, A. Simmonett and H. F. Schaefer, *Mol. Phys.*, 2012, **110**, 2419–2427.

63 T.-L. Tso and E. K. C. Lee, *J. Phys. Chem.*, 1984, **88**, 5475–5482.

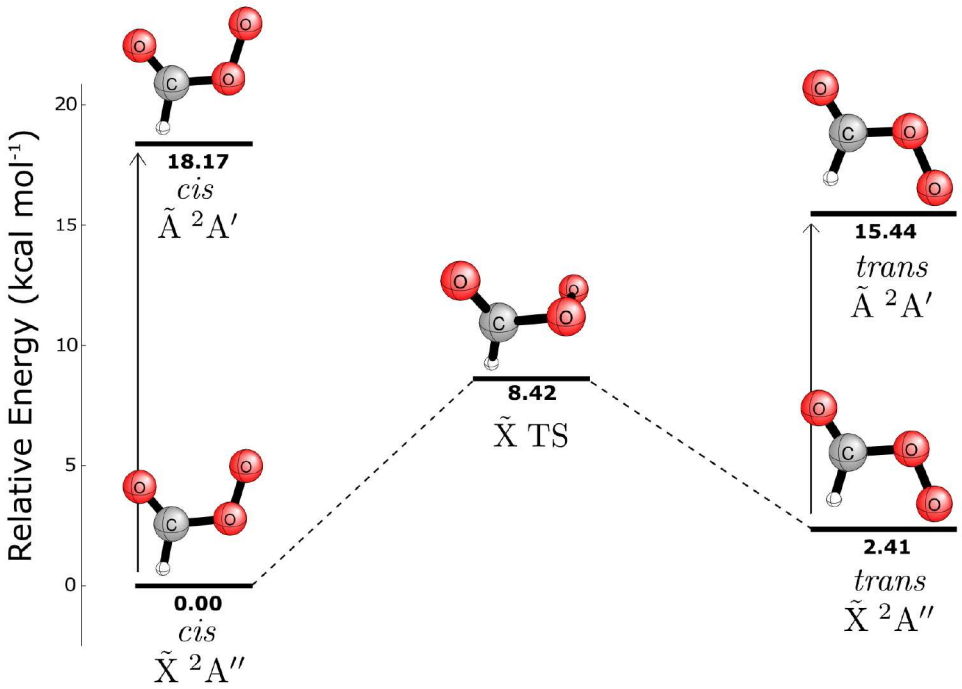

Acylperoxy radicals [RC(O)OO•] play an important catalytic role in many atmospheric and combustion reactions. Accordingly, the prototypical formylperoxy radical [HC(O)OO•] is characterized here using high-level *ab initio* coupled-cluster theory. Important experiments have been carried out on this system, but have not comprehensively described the properties of even the ground electronic state. We report *cis* and *trans* geometries for the ground ($\tilde{X}\,^2A''$) and first excited ($\tilde{A}\,^2A'$) state equilibrium conformers and the torsional saddle point on the ground state surface at the CCSD(T)/ANO2 level of theory. Relative energies of these ground- and excited-state stationary points were obtained using coupled cluster theory with up to perturbative quadruple excitations, extrapolated from the sextuple zeta basis set to the complete basis set limit. These methods predict conformational energy differences $\Delta E(trans\text{-}\tilde{X} \rightarrow cis\text{-}\tilde{X}) = 2.35$ kcal mol^{-1} and $\Delta E(trans\text{-}\tilde{A} \rightarrow cis\text{-}\tilde{A}) = -2.95$ kcal mol^{-1}. On the $\tilde{X}$ surface, the transition state for the conformational change lies 8.42 kcal mol^{-1} above the *trans* ground state minima. The adiabatic electronic excitation energies from the ground state isomers are predicted to be 18.17 ± 0.10 (*trans*) and 13.03 ± 0.10 kcal mol^{-1} (*cis*). The former is in excellent agreement with the 18.1 ± 1.4 kcal mol^{-1} transition found by Lineberger and coworkers. Additionally, transition properties between the $\tilde{X}\,^2A''$ and $\tilde{A}\,^2A'$ states are reported for the first time, using the equation of motion (EOM)-CCSD method, which predicts lifetimes for *trans*-$\tilde{A}\,^2A'$ HC(O)OO• of 5.4 ms and *cis*-$\tilde{A}\,^2A'$ HC(O)OO• of 20.5 ms. Second-order vibrational perturbation theory was utilized to determine the fundamental frequencies at the CCSD(T)/ANO2 level of theory for the *cis* and *trans* conformers of the $\tilde{X}$ and $\tilde{A}$ states and five ground state isotopologues of both conformers: $H^{13}C(O)OO^{\bullet}$, $HC(^{18}O)OO^{\bullet}$, $HC(O)^{18}O^{18}O^{\bullet}$, $DC(O)OO^{\bullet}$, and $DC(O)^{18}O^{18}O^{\bullet}$. This study provides high accuracy predictions of vibrational frequencies, helping to resolve large uncertainties and disagreements in the experimental values. Furthermore, we characterize experimentally unassigned vibrational frequencies and transition properties.